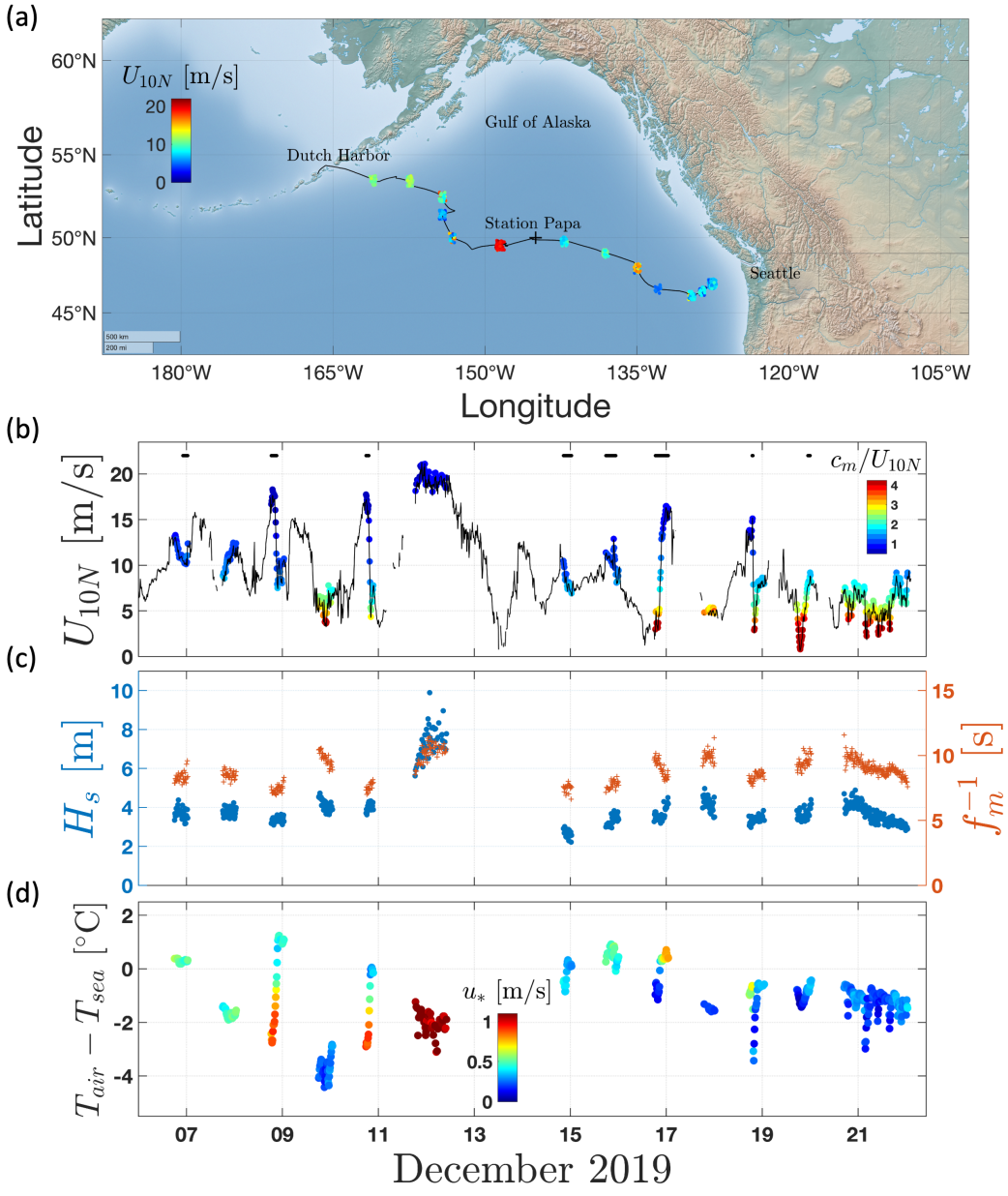

Figure A.1: Overview of (a) the cruise track (solid line) and average location of the drifting SWIFT buoys (circles) during each deployment along the transit, and $(b-d)$ the observed range of environmental conditions. Here U_{10N}, H_s, f_m, T_{air}, and T_{sea} represent 10-minute average neutral wind speed at 10 m above the sea surface, significant wave height, spectrally-averaged wave frequency, and air and water temperature, respectively. The color code in (b) and (d) shows the wave age and the air-side friction velocity, respectively. In (b), the horizontal line segments indicate the intervals during which data were collected in the presence of persistent rain (rain rates have not been measured). Local water depths during most of the deployments were greater than 4000 m.

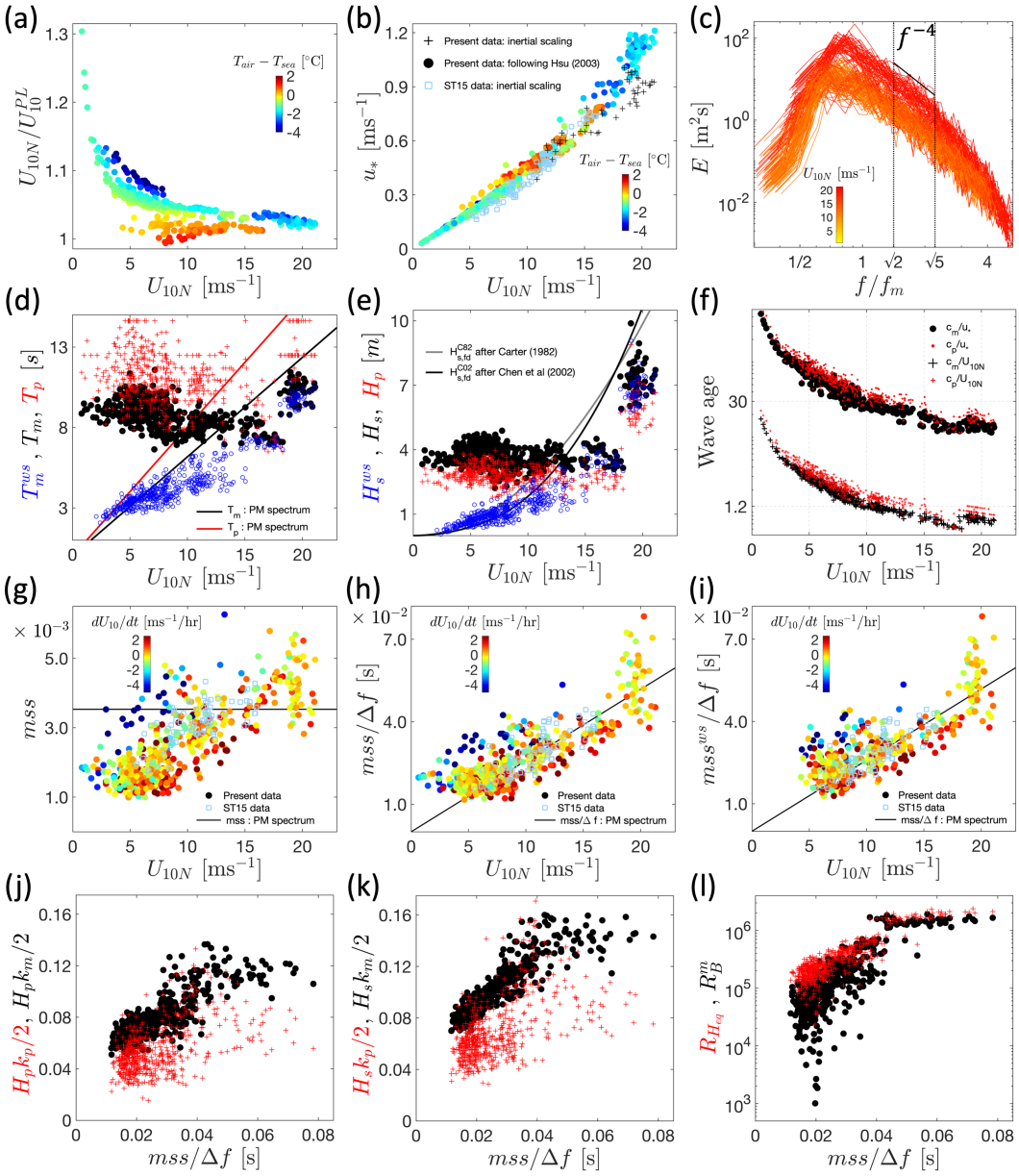

Figure A.2: Observed range of wind and wave statistics against U_{10N} and equilibrium-range mean square slope $mss/\Delta f$ (Eq. 2). All variables are defined in §2.2 and §2.3.

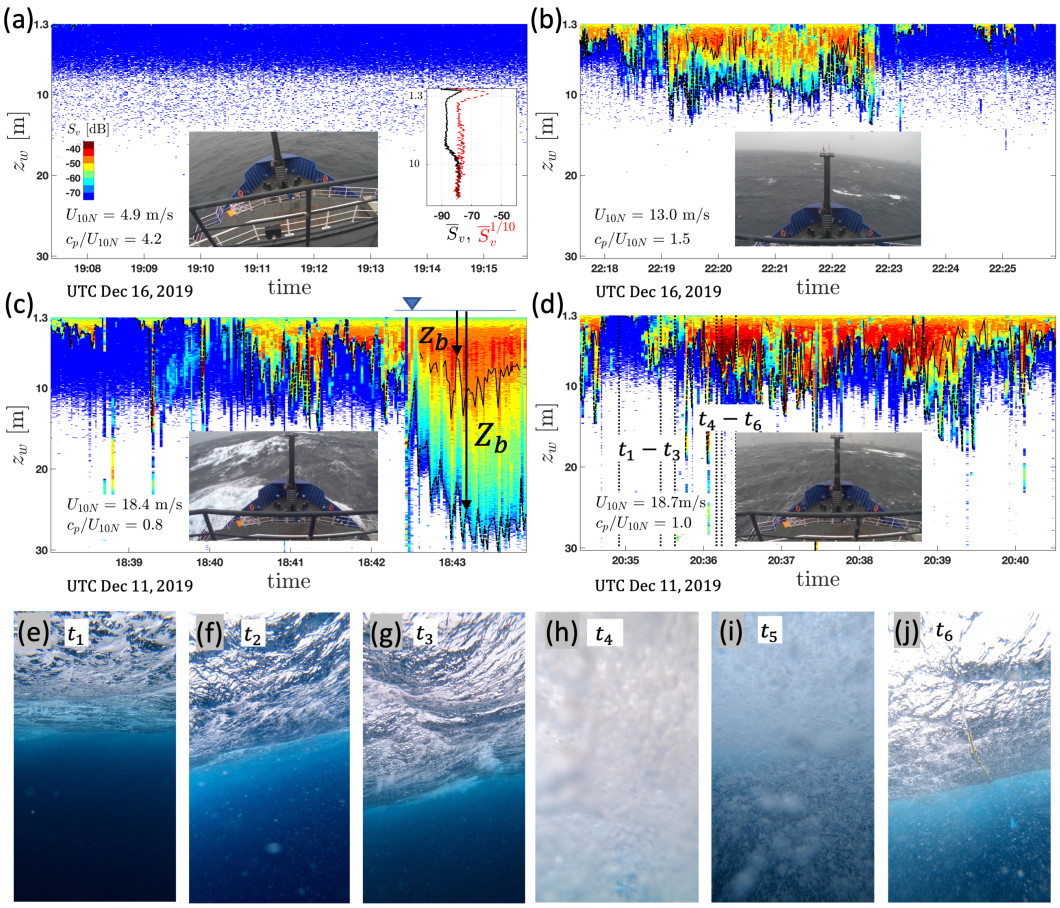

Figure A.3: Examples of a depth-time map (echogram) of the volume backscattering strength S_v [dB] in $(a - b)$ a rapidly evolving sea with different sea state conditions (but steady rain) on UTC Dec 16 and in $(c-d)$ a storm with sustained wind speeds of $U_{10N} > 18.0$ ms^{-1} on UTC Dec 11. In (a), the signal represents observations just after a steady calm sea state with minimum whitecapping and is expected to be mainly from scattering particles or bubbles not associated with breaking waves. The sub-surface optical images in $(e - j)$ correspond to the time instants $t_1 - t_6$ marked by the vertical dashed lines in (d) and are collected by a GoPro camera mounted on the SWIFT buoy. Above-surface optical images in $(a-d)$, taken from a camera on the ship's bridge, show a snapshot of the surface wave field within the time range of the corresponding echogram. Dotted-dashed and solid contours indicate Z_b and z_b, the two estimates of the local penetration depth of entrained bubbles defined in § 2.5. Echograms are collected by a downward-looking echosounder integrated on SWIFT buoys in a surface-following reference frame z_w, where z_w is positive downward, and $z_w = 0$ represents the instantaneous free surface level.

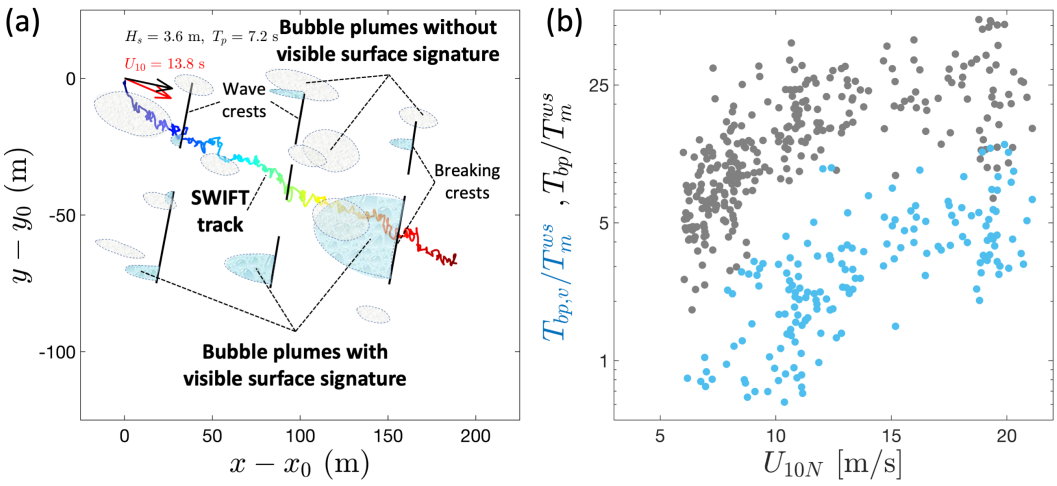

Figure A.4: (a) Schematic of a SWIFT track (with respect to the earth frame) drifting across an intermittent field of bubble clouds during a 512-s burst, along which echogram data are collected in a surface following reference frame, and (b) apparent residence time of bubble clouds in echogram data against wind speeds. In (a), (x_0, y_0) is the initial horizontal location of the buoy, and the black and red arrows show the dominant wave and wind directions, respectively. Subscripts bp and bp, v denote the statistics corresponding to the bubble plumes obtained from the thresholding methods BDM1 and BDM2 (described in §2.5), respectively.

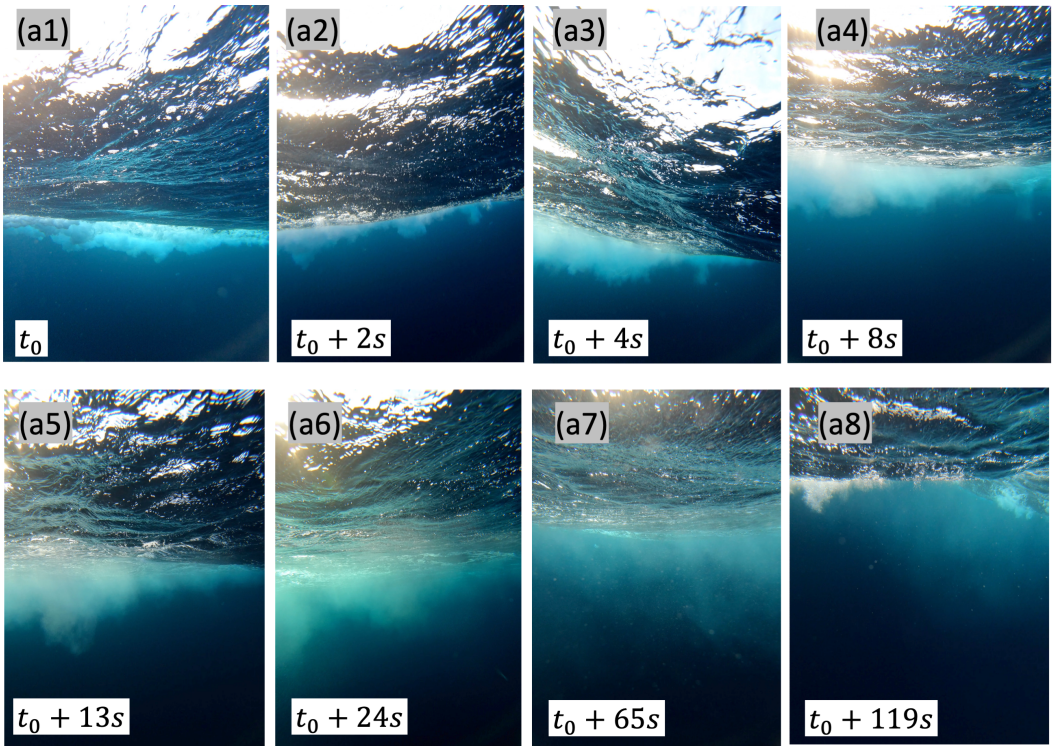

Figure A.5: Example sub-surface images collected by a GoPro camera on a SWIFT buoy showing the sub-surface visible signature of an evolving bubble plume in an old sea with moderate wind speeds of $U_{10N} \approx 11$ ms^{-1}.

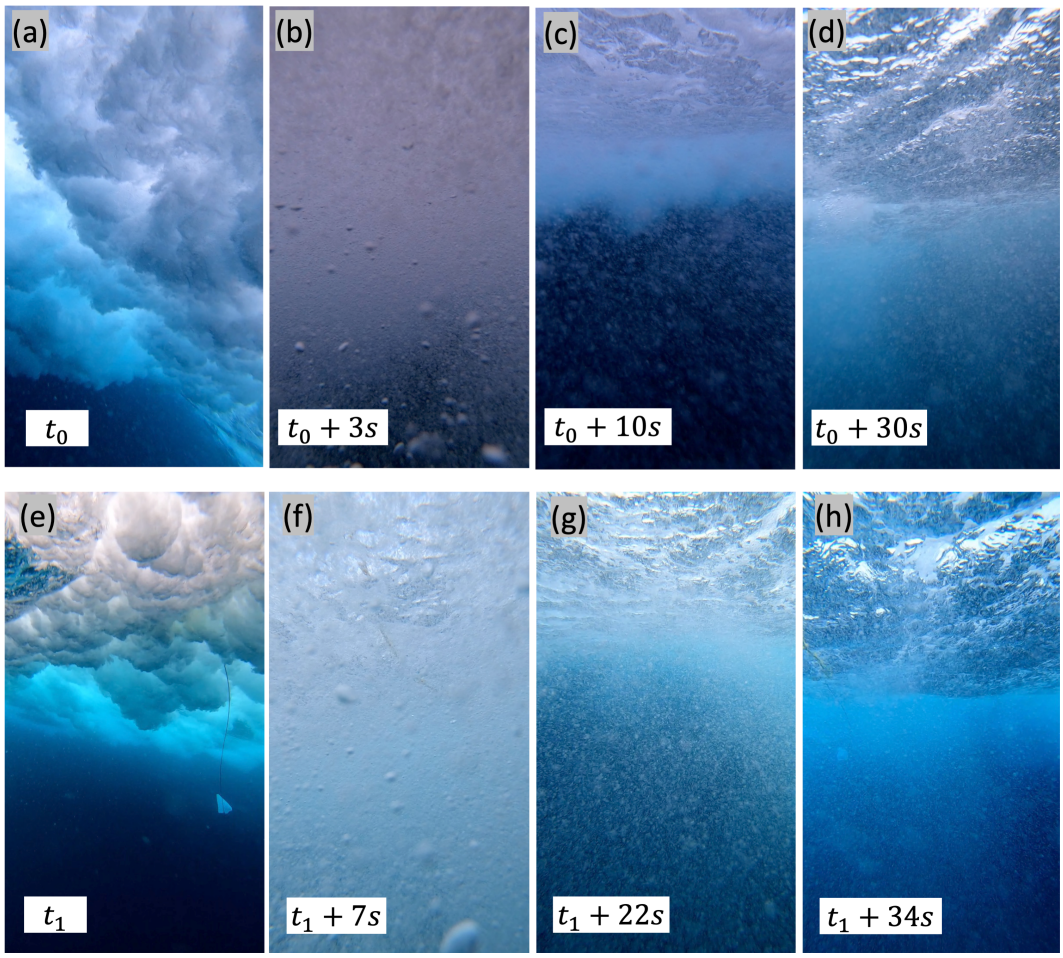

Figure A.6: Example sub-surface images collected by a GoPro camera on a SWIFT buoy showing the sub-surface visible signature of two different evolving bubble plumes in a storm with sustained wind speeds of $U_{10N} > 18$ ms^{-1}.

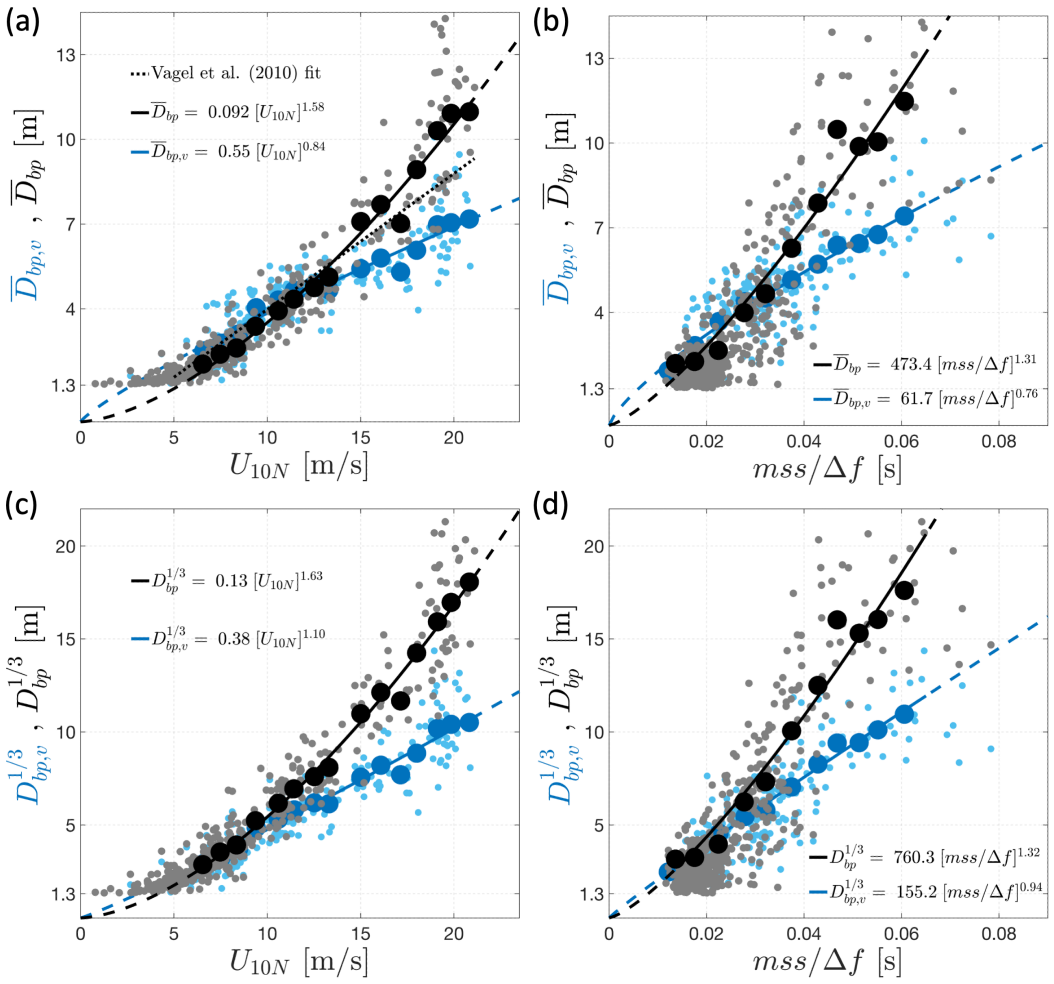

Figure A.7: Observed range of $(a - b)$ mean (Eq. 6) and $(c - d)$ significant (Eq. 7) bubble plume depths against wind speed U_{10N} and the equilibrium range $mss/\Delta f$. Fits are obtained from the least squares fitting to the binned data points (large circles). Subscripts bp and bp, v denote the statistics corresponding to the bubble plumes obtained from the thresholding methods BDM1 and BDM2 (described in §2.5), respectively.

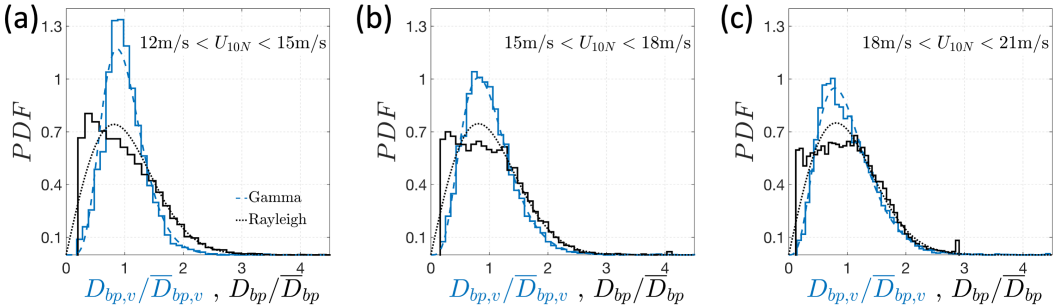

Figure A.8: Probability distribution function, PDF, of the estimated bubble depths at different wind speed ranges. Dotted and dashed lines show the fitted Rayleigh and Gamma distributions to the observed PDFs.

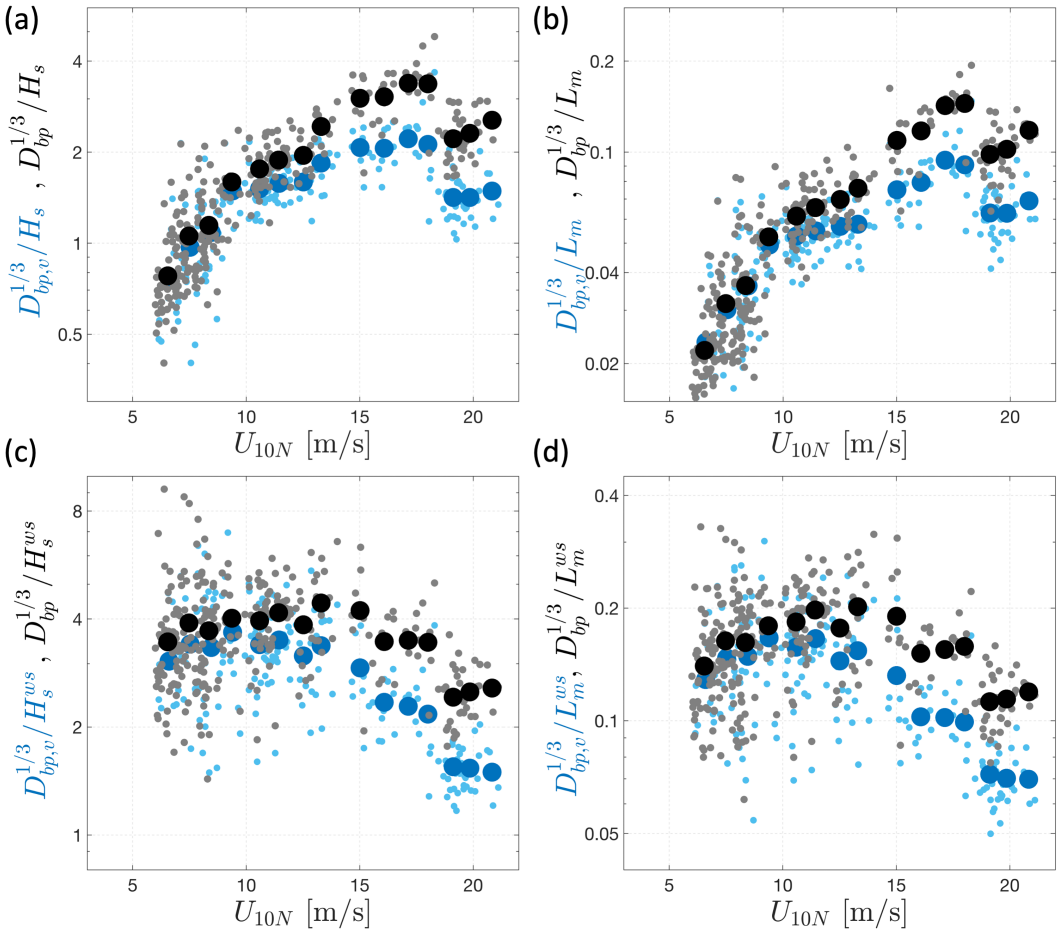

Figure A.9: Scaled bubble plume penetration depths against wind speeds. Here H_s is the total significant wave height, $L_m = g/2\pi * T_m^2$ is the total mean wavelength, H_s^{ws} is the wind sea significant wave height, $L_m^{ws} = g/2\pi * (T_m^{ws})^2$ is the wind sea mean wavelength, all defined in §2.3. Large circles represent the binned data points. Subscripts bp and bp, v denote statistics correspond to the bubble plumes obtained from the thresholding methods BDM1 and BDM2 (described in §2.5), respectively.

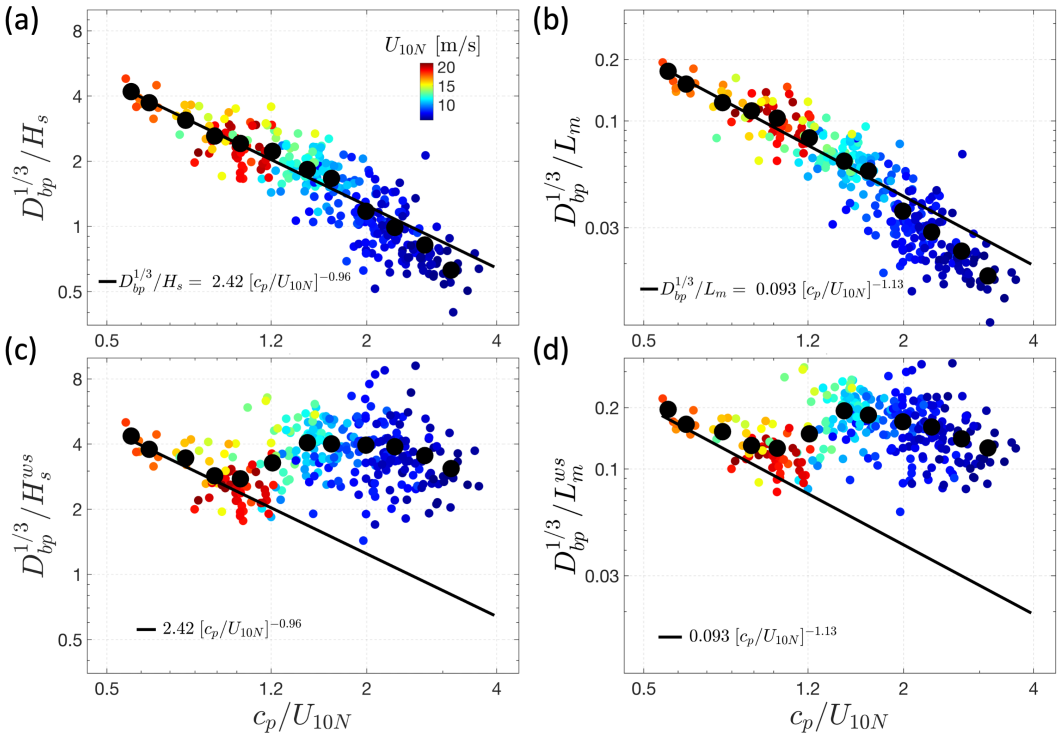

Figure A.10: Scaled bubble plume depths against wave age colored by wind speed. In (a) and (b), the fits are obtained from the least squares fitting to the binned data points (large circles). Definitions are as in Figure A.9.

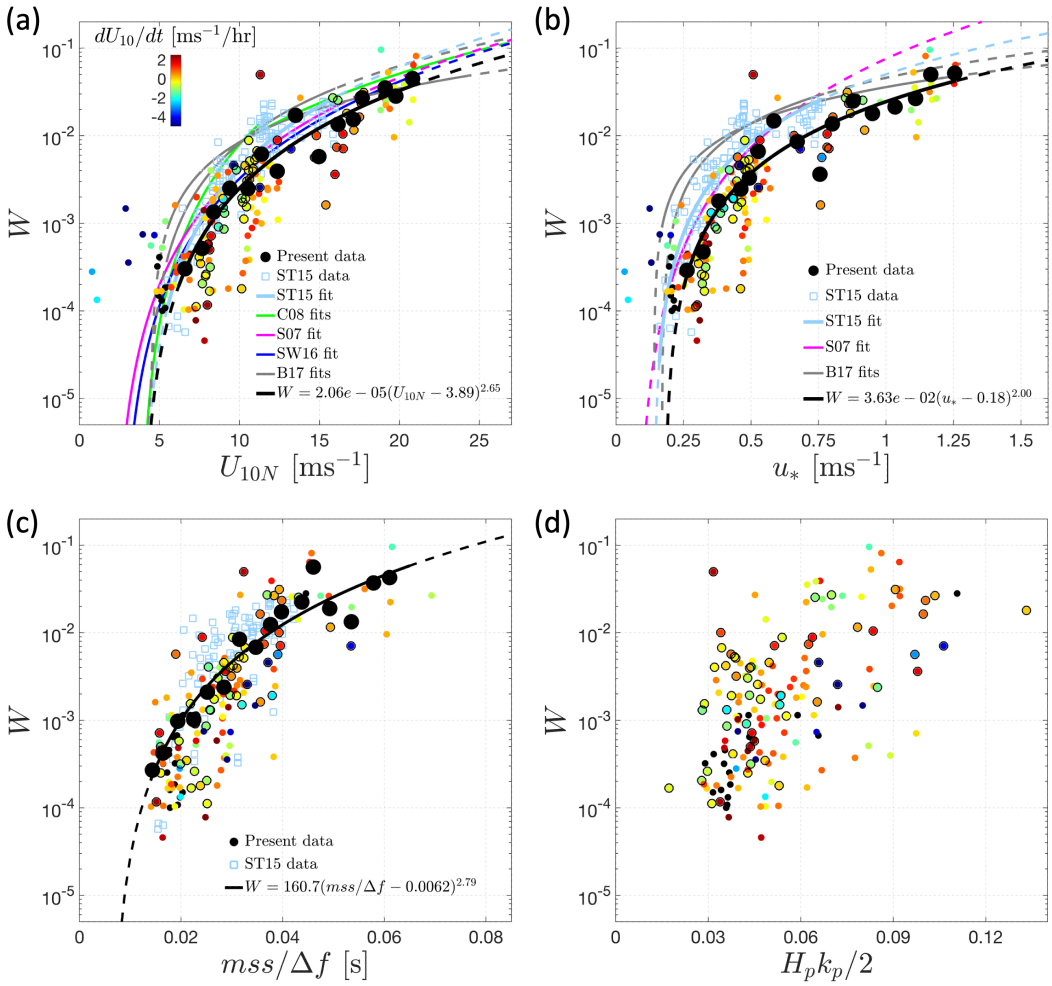

Figure A.11: Observed range of whitecap coverage against (a) wind speed U_{10N}, (b) air friction velocity u_*, (c) the equilibrium range $mss/\Delta f$, and (d) the significant spectral peak steepness $H_p k_p/2$, all colored by the wind accelerations dU_{10N}/dt (all defined in §2). Circles with black edges represent the data in the presence of rain (rain rates have not been measured). The best fits to the present data are obtained from the least squares fitting to the bin-averaged data points (large black circles).

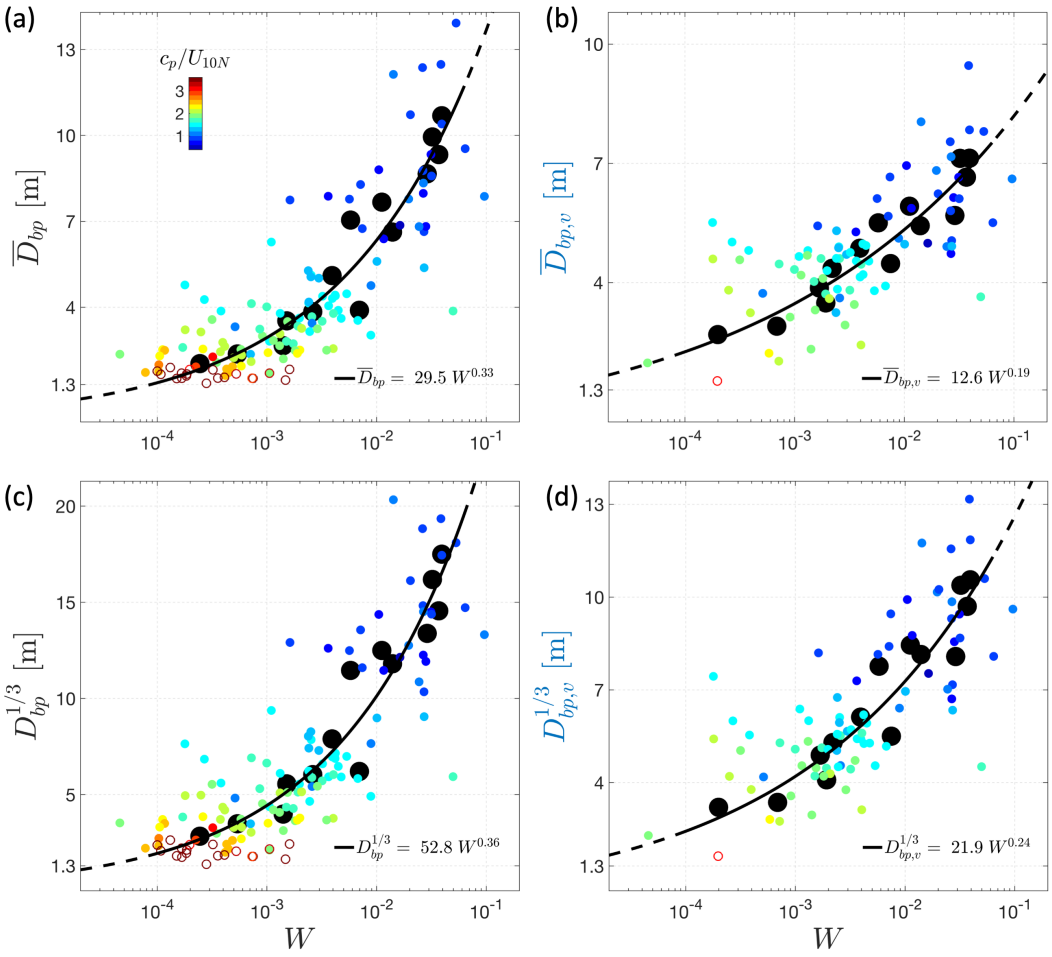

Figure A.12: Mean and significant bubble plume depths against whitecap coverage. The best fits to the present data are obtained from the least squares fitting to the bin-averaged data points as a function of U_{10N} (large black circles). Open circles represent the data with $U_{10N} < 6$ ms^{-1}.

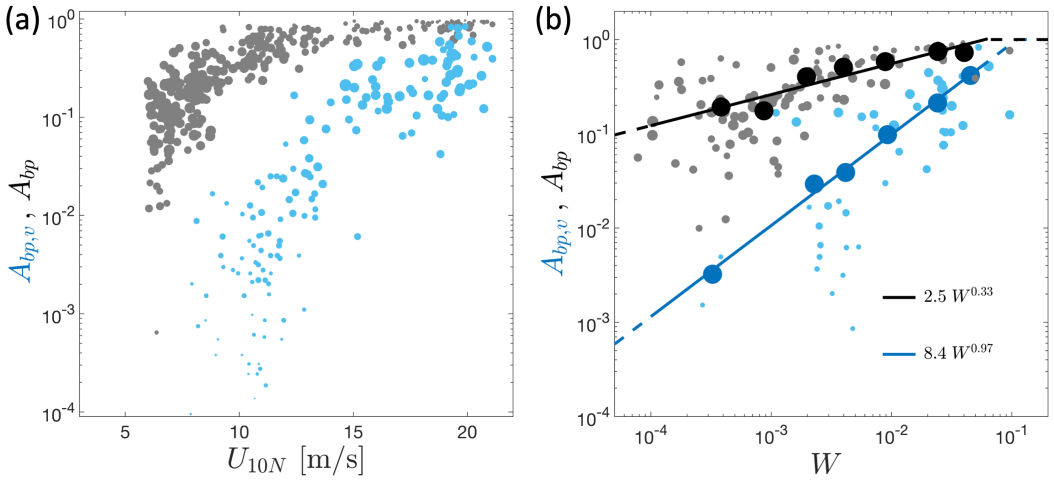

Figure A.13: Proxy for the fractional area of the bubble plumes against (a) wind speed and (b) whitecap coverage. Symbol sizes are a function of the number of bubble clouds detected in a burst averaged over concurrent (1 to 4) bursts ranging from 0.5 to 26. In (b), large symbols represent the corresponding binned data with more than three detected bubble clouds in a burst. Subscripts bp and bp, v denote the statistics corresponding to the bubble plumes obtained from the thresholding methods BDM1 and BDM2 (described in §2.5), respectively.